IOP PUBLISHING SCIENCE AND TECHNOLOGY OF ADVANCED MATERIALS

Sci. Technol. Adv. Mater. **10** (2009) 034502 (9pp) doi:10.1088/1468-6996/10/3/034502

TOPICAL REVIEW

3D heterostructures and systems for novel MEMS/NEMS

Victor Yakovlevich Prinz, Vladimir Alexandrovich Seleznev, Alexander Victorovich Prinz and Alexander Vladimirovich Kopylov

Institute of Semiconductor Physics, Russian Academy of Sciences, Siberian Branch, Lavrent'ev Avenue 13, Novosibirsk 630090, Russia

E-mail: prinz@isp.nsc.ru

Received 21 January 2009
Accepted for publication 24 May 2009
Published 14 July 2009
Online at stacks.iop.org/STAM/10/034502

Abstract

In this review, we consider the application of solid micro- and nanostructures of various shapes as building blocks for micro-electro-mechanical or nano-electro-mechanical systems (MEMS/NEMS). We provide examples of practical applications of structures created by MEMS/NEMS fabrication. Novel devices are briefly described, such as a high-power electrostatic nanoactuator, a fast-response tubular anemometer for measuring gas and liquid flows, a nanoprinter, a nanosyringe and optical MEMS/NEMS. The prospects are described for achieving NEMS with tunable quantum properties.

Keywords: micro-electro-mechanical systems (MEMS), nano-electro-mechanical systems (NEMS), MEMS/NEMS heterostructures

(Some figures in this article are in colour only in the electronic version)

1. Introduction

Micro-electro-mechanical systems (MEMS) are a well-established R&D field. Fabrication methods for MEMS building blocks and various applications of MEMS have been described in detail in numerous publications (see [1–4], for instance). In terms of fabrication, MEMS are currently dominated by planar processing techniques, which are based on silicon integrated circuit (IC) technology. The planar approach and the strong dependence on silicon worked well in the early years because many processing tools and methodologies that are commonly used in IC fabrication could be directly applied for the fabrication of MEMS devices. The considerable progress in MEMS was due to the full exploitation of the mechanical degree of freedom and the evolution to 3D structures. Here, bulk micromachining, surface micromachining and LIGA (from German: Lithographie, Galvanoformung, Abformung) technologies have contributed substantially to the already existing possibilities [5]. Structures fabricated by these processes include comb electrostatic actuators. Other well-known applications of such processes include MEMS cavities in inkjet printers and MEMS sensors in automobiles [2].

Presently, we are witnessing a transition from MEMS to nano-electro-mechanical systems (NEMS) that offer new exciting applications [3, 4]. In the transition from MEMS to NEMS, the feature sizes are reduced, making the fabrication methods previously developed for MEMS unsuitable for the production of high-precision NEMS elements. On the other hand, nanomechanical devices require precise 3D nanostructures whose parts move at nanometer scale. The key challenge in NEMS is therefore the development of new methods for routine reproducible nanofabrication.

Several approaches to solving this problem are presently available. For instance, 3D nanostructures have been fabricated using a focused electron beam [6]. Electron-beam-induced deposition is a promising technique for maskless nanofabrication that has been studied by many researchers because of its higher resolution due to the smaller beam spot, and because of the possibility of combining

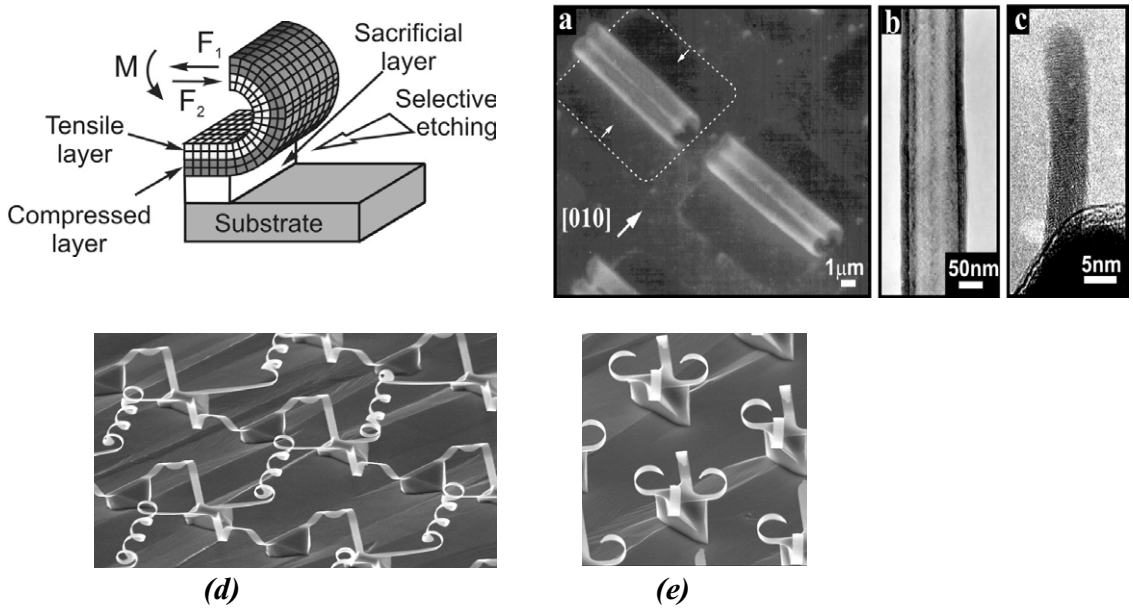

Figure 1. Schematic illustration of the strain-driven fabrication of shells. The interatomic elastic forces in the lower layer (F1) and the upper layer (F2) are oppositely directed, giving rise to a nonzero moment of forces M. Under the action of this moment, the initially planar bilayer bends or rolls up into the shape of a scroll [7]. Scanning electron microscopy (SEM; a, d, e) and high-resolution transmission electron microscopy (HRTEM; b, c) images of rolled-up InGaAs/GaAs nanotubes formed from bilayered films [7]. (d) and (e) InGaAs/GaAs 3D open shells obtained by lithography and directional rolling [9].

top-down and bottom-up approaches. There is no doubt that this technique, enabling the fabrication of many 3D structures, will be widely used. This method can also be used as a supplementary tool. It should be noted, however, that this approach uses a successive process; as a result, the time necessary for batch nanofabrication may become unacceptably long.

It is therefore acutely recognized that a parallel process for fabricating 3D nanostructures is required, ensuring nanoscale sizes and near-atomic precision in fabricated NEMS. In addition, efficient nanotechnology should be applicable to various materials and allow the formation of variously shaped, scalable structures necessary for practical applications. Such technology should also be robust and compatible with the well-established procedures for the epitaxial growth of nanostructures, as well as with planar processing techniques, and should use already existing plants and facilities. To meet these requirements, a technology has been introduced [7–9] that enables the formation of precise 3D shell nanostructures of various shapes. This technology has been used to fabricate tubes with diameters down to 2 nm, helices with diameters down to 7 nm, and periodically corrugated structures with corrugation periods down to 10 nm. It has been demonstrated to be suitable for the batch production of precise 3D structures for use in NEMS.

The new technology is based on the use of high-precision initial plane structures and systems, and also on the use of self-forming and self-assembling processes for the fabrication of precise 3D objects capable of executing mechanical motion, elastically changing their shape and so forth [7, 8]. In [8], a new concept of fabricating building blocks for nanoelectronic and nanomechanic devices was discussed. In the present paper, we summarize the results obtained in the pilot development of MEMS and NEMS, and show how the proposed concept can be used in the formation of building blocks for micro- and nanomechanical devices. The examples of building blocks and experimental structures given in this paper merely illustrate the simplest 3D structures. The next developmental stage in this field will be the adaptation of this technology to the fabrication of multilayered 3D structures and materials.

2. Fabrication principles and classification of structures

For high-performance MEMS/NEMS, 3D structures are required to exhibit the free motion of their parts. Such structures must be fabricated with high precision. However, until recently no standard processes were available for fabricating 3D building blocks with atomic or nanometer accuracy. In recent years, there has been a clear tendency towards the use of 3D rather than planar building blocks [5]. Another tendency, towards using new materials in MEMS, was discussed in detail in [10, 11]. The previously used approaches were primarily based on LIGA technology which has contributed greatly to the formation of 3D MEMS microstructures. LIGA processes, however, are restricted to micrometer sizes, whereas the precision of NEMS fabrication must be of nanometer or atomic scale [2].

The general approach to the formation of semiconductor nanotubes and other 3D nanoshells [7–9] is illustrated in figures 1 and 2. The initial structure includes a sacrificial layer and a bilayered heterofilm that is strained as a result of the lattice mismatch with the substrate. After selective removal of the sacrificial layer, the strained heterofilm bends,

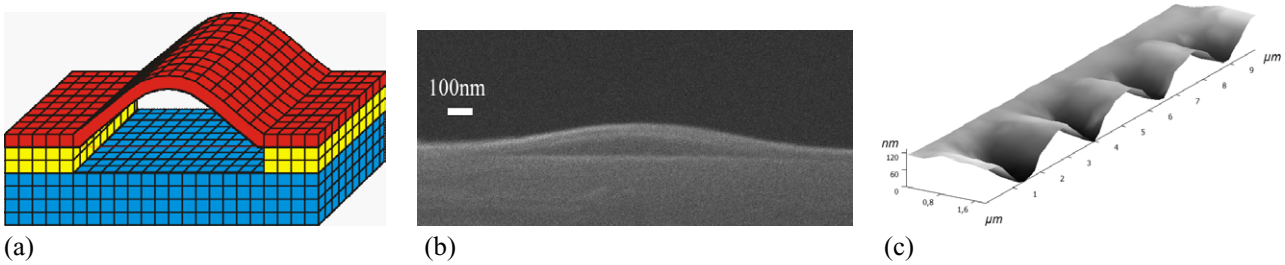

(a) (b) (c)

Figure 2. (a) Schematic illustration of buckling of compressed layer after its partial detachment from the substrate resulting from selective etching of the underlying AlAs sacrificial layer. (b) SEM cross-sectional images of buckled and corrugated InGaAs–GaAs structures [8]. (c) 3D image of SiGe/Si corrugated film obtained using atomic force microscopy [12].

rolls, or buckles because of internal elastic forces, forming the final elastic shell structure. The curvature radius of the final 3D shell is precisely defined by the mechanical strain and by the thicknesses of the constituent layers in the initial planar structure. In the simple case of an initial planar bilayer structure we have

$$R = \frac{2}{3} d \frac{a}{\Delta a}, \tag{1}$$

where d is the thickness of each layer and $\Delta a/a$ is the lattice mismatch between the layers. The thicknesses of the layers, as well as the mechanical strain induced by the lattice mismatch between the layers, can be controlled with extreme precision, thus enabling precise control of the curvature radius from one nanometer to hundreds of micrometers (for a review, see [8, 9]). A great variety of shell designs have now been demonstrated, and many other configurations can be formed on one substrate. Semiconductors, metals, or dielectrics can be used as materials for this technology.

Figure 1 illustrates closed shells (a–c) and open shells (d, e) fabricated in the described manner. Open shells are very sensitive to mechanical forces, whereas closed shells were found to be extremely rigid. Our experiments showed that InGaAs/GaAs tubes (closed shells) of 1 μm diameter, 10 nm wall thickness and 100 μm length can be elastically loaded with a force of 0.1 N [7].

The formation of nanobuckles and the possibility of controlling their dimensional parameters were first demonstrated in [8]. The fabricated nanocorrugated systems had periods of up to 10 nm [8, 9]. Figure 2 illustrates a nanocorrugated (nanobuckled) film prepared from a compressed, initially flat film locally detached from a substrate. Such corrugations can be formed because locally released compressed planar films are unstable and tend to buckle. The buckled shape results from the simple elongation of the released films in the direction along the edge [12]. This technology is being further developed by many research groups [13–15].

The fabrication technology includes the following critical points: (i) the highly selective etching of sacrificial layers [7]; (ii) the directional rolling up of films, yielding 3D micro- and nanoshells of various shapes [16–18]; (iii) the assembly of micro- and nanoshells into more complex architectures [19]; (iv) the super-critical drying of nanoshells [20]; and (v) the formation of nanoshells whose sizes can be precisely controlled in three dimensions [21].

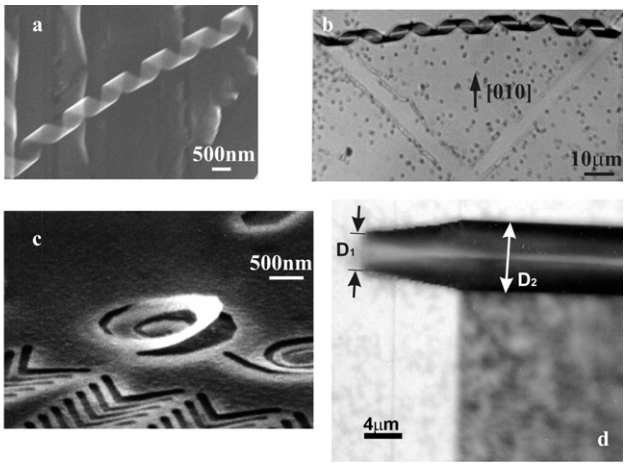

Figure 3. Different spiral configurations obtained from strained films using self-forming processes. (a) Helix prepared from straight Si/SiGe strips. (b) Joint left- and right-handed spirals attached to a substrate at their ends. The spirals, which were obtained from a V-shaped mesastructure, rolled up away from its apical corner [17]. (c) Archimedean spiral; the film lifted from the substrate by the internal elastic strain in the SiGe film [16]. (d) 40-turn telescopic spiral [8].

This fabrication technology, which is fully compatible with IC technology, uses the advantages of the well-established planar technology and the high atomic precision of epitaxial growth processes used to grow strained monolayers. Several examples of applications of this fabrication technology are given below, illustrating the possibility of fabricating many novel MEMS and NEMS devices.

We illustrate the rich variety of shell shapes and their great potential for application to MEMS/NEMS by focusing on springs, which are often used as the building blocks of MEMS/NEMS. Figure 3 shows four different spiral configurations obtained from strained films using self-forming processes. Figure 3(a) shows spiral structures prepared from straight Si/SiGe strips deflected away from the direction of the minimum Young's modulus on the film crystal surface. Figure 3(b) shows joint left- and right-handed spirals attached to a substrate at their ends; here, the spirals, which were obtained from a V-shaped mesa structure, were rolled up away from the apical corner of the mesa structure. Figure 3(c) shows an Archimedean spiral; the film was lifted from the substrate by the internal elastic strain in the SiGe film. Figure 3(d) shows a 40-turn telescopic spiral. Such structures

can also be obtained from a film with thickness gradient along the strip, which results in a gradient of curvature radius along the surface. Figures 1(d) and 1(e) show a system of spirals also prepared from a system of strips. It is possible to fabricate a variable-pitch, variable-diameter spiral from a bilayer film with variable thickness of the top layer; in this case, the elastic force bending the film also varies along the surface. These simplest 3D shells can be used in actuators, such as those described in [22], and sensors, including the supersensitive sensors described in [23]. It should be noted that such shells can be formed from many materials, including semiconductors, dielectrics and metals. Of prime importance here are shells formed from hybrid films and shells in which semiconductor layers are used as shape-generating elements.

In addition, this technology is ideal for the formation of NEMS owing to the following features. Firstly, it is scalable down to nanometer dimensions, enabling the formation of shells with molecular- and atomic-level thicknesses. Secondly, this technology allows shell fabrication with high precision. Thirdly, it is perfectly compatible with the well-established planar lithographic technology used for ICs. Fourthly, it allows to produce a rich variety of shell shapes made of various materials. This technology, initially developed for the formation of semiconductor micro- and nanoshells, has subsequently been extended to the formation of hybrid metal-semiconductor shells [24], metal micro- and nanoshells [25], organic nanoshells [26] and metal shells formed from strained layers deposited onto polymer films [27]; these processes offer additional possibilities in nanofabrication.

The developed technology meets all the requirements for NEMS fabrication and offer high performance for the fabrication of freestanding, multilayered and self-assembling structures.

3. Novel micro- and nanoactuators

Nowadays, the fabrication of solid-state nanoactuators is still a challenging problem, and active research to find new approaches towards solving this problem is under way.

The rich variety of shapes offered by elastic shells formed from strained films of many materials opens up wide possibilities for the creation of various micro- and nanoactuators and sensors. A simple artificial actuator developed around spiral shells is given as an example [22]. The proposed structure allows the development of self-propelled devices and swimming microrobots, which mimic bacterial flagella in both size and motion. The swimmer consists of an InGaAs/GaAs or InGaAs/GaAs/Cr helical tail and a thin soft-magnetic head. These magnetically driven helical devices can be used as wireless manipulators for medical and biological applications under three-dimensional control in fluid environments [23, 28]. In [27], a catalytic tubular microjet is described, which was rolled up from a Ti/Fe/Au/Ag multilayer nanomembrane. Inside the microjet, hydrogen peroxide (H_2O_2) is decomposed into O_2 bubbles and water by a catalytic reaction of H_2O_2 with the inner Ag nanotube wall.

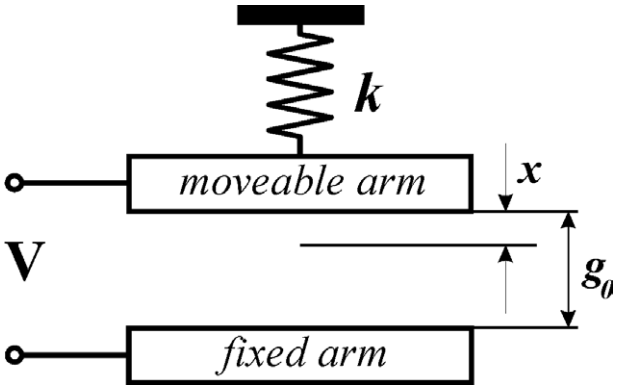

Figure 4. Schematic of a simple electrostatic capacitor actuator.

The simplest and most widespread actuators use the electrostatic attraction force acting between two parallel plates (usually, one plate is fixed and the other is moving). Electrostatic micro- and nanoactuators are easy to design and fabricate, and they are easily integrated in micro- and nanosystems. They are applied in radio engineering as active filters or resonators, and also in hydrodynamic systems. They can be employed as pumps for liquids or finely dispersed materials, as atomizers for liquid droplets, and also as accelerometers and sensors in many industries. These electrostatic nanoactuators are very promising owing to the high energy density accumulated in these devices and the large force that they can generate. These factors are particularly advantageous in scaling the separation between the plates down to nanometer dimensions. The high accuracy desired in the formation of such super narrow nanogaps can be achieved by molecular-beam epitaxy, which can yield structures with perfectly controlled separation between the layers. A disadvantage of such actuators is their insufficient stability: they suffer from pull-in phenomena [29, 30]. Moreover, the range of stable displacements in such actuators is much smaller than the initial separation between the electrodes.

Let us consider an electrostatic actuator formed by two parallel plates of area A with separation g_0 between the plates (figure 4). Neglecting edge phenomena, the energy accumulated in such an actuator–capacitor is defined by the voltage V applied to the plate electrodes and by the capacitance C of the capacitor:

$$W = \frac{1}{2}CV^2 = \frac{\varepsilon_0 A V^2}{2g_0}. \tag{2}$$

The force acting between the plates is

$$F = \frac{\mathrm{d}W}{\mathrm{d}g} = \frac{\varepsilon_0 A V^2}{2g_0^2}. \tag{3}$$

Thus, the force F is a nonlinear function of the potential and of the separation between the plates. For such a system to act as an actuator, one or both plates should be movable and fixed to an elastic compensator. A spring [31–34] or a viscous liquid [35] can be used as the compensator. The system is

at equilibrium when the elastic force due to the spring is balanced by the electrostatic attracting force:

$$kx = \frac{\varepsilon_0 A V^2}{2(g_0 - x)^2}. \quad (4)$$

Here, kx is the elastic force generated by the spring, and the right-hand side is the electrostatic attraction force. The elastic force varies linearly with x, whereas the electrostatic force is nonlinear with respect to x. An equilibrium state of the system is only possible if the electrostatic force is less than or equal to the elastic force. At some voltage $V_{\text{pull-in}}$ the electrostatic force becomes greater than the elastic force, the system becomes unstable and the capacitor plates come in contact. Normally, such a state emerges at $x \approx 0.3g_0$; this means that the controlled electrostatic force developed in the actuator is almost 50 times smaller than the force that would be developed in the case of $x \approx 0.9g_0$ (see the formula above). The pull-in effect is the main shortcoming of capacitor systems because it strongly limits the range of displacements and the force generated in the actuator. Various liquids can be used to avoid this effect [35]. However, this results in the catastrophic deterioration of all performance characteristics of the actuator.

In [36, 37], we proposed an alternative electrostatic actuator without this shortcoming. In the new actuator, an elastic corrugated film, acting as a variable-rigidity spring, is installed between the two parallel plates. As the bias voltage applied to the electrodes increases, the corrugated film deforms and switches between states with a consecutively increasing number of corrugation periods and decreasing corrugation amplitude (see figure 5). This allows us to obtain nanogaps between electrodes and to dramatically increase the electrostatic attraction. It should be noted that as the electrodes approach each other, both the attractive force and the actuator power increase (the electrostatic force is inversely proportional to the square of the separation between the plates). A specific feature of corrugated nanofilms is their ability to withstand enormous mechanical stresses [12]. Upon removing the voltage, the actuator, after passing through intermediate successive states, reacquires its initial configuration. Numerical calculations and experimental tests have shown that such variable-rigidity actuators, which have a considerable range of displacements, are capable of generating forces of up of to $10^5\,\text{N cm}^{-2}$ [36, 37].

Such actuators were experimentally realized with a GaAs/AlAs/InGaAs/AlAs/GaAs structure and a hybrid structure (substrate/corrugated film/ferroelectric film/semiconductor film). Special monolayer coatings were used to prevent sticking. For Si/SiGe/Si structures, we used 1-octadecene monolayers [38]. The tests were performed using capacitance methods for measuring the separation between the electrodes. The small dimensions of the actuator and the possibility of low control voltages (< 5 V at a 100 nm initial gap and 6 nm thickness of the corrugated film) make the device promising for nanoscale applications.

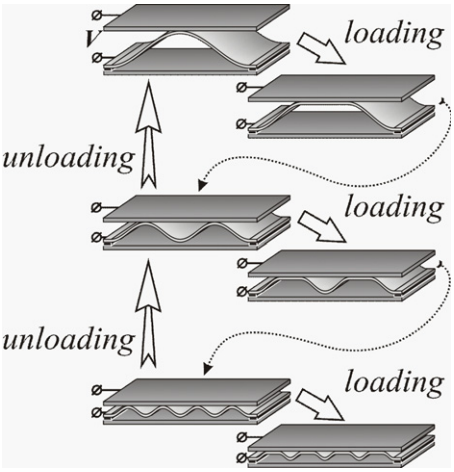

(a)

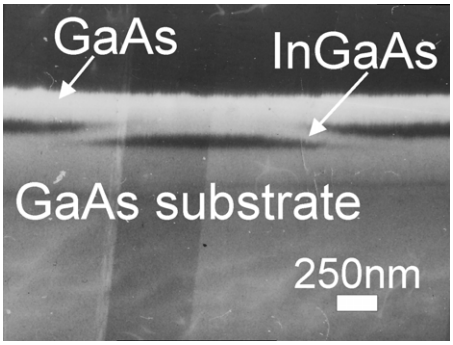

(b)

Figure 5. (a) Schematic illustration of the operating sequence of a variable-rigidity actuator. An increase in the bias voltage leads to an increased load acting on the corrugated film, causing the film to sequentially switch into states with a greater number of periods and smaller corrugation amplitude (from top to bottom). The upward arrows show the reverse process upon decreasing the bias voltage. (b) Cross-sectional view of an experimental actuator structure fabricated from an initial GaAs/AlAs/InGaAs/AlAs/GaAs structure by etching the AlAs sacrificial layer [36, 37].

4. Hot-tube sensors as basic elements for smart control of turbulence systems

The nanometer thicknesses of micro- and nanoshells, the high stability and precision of their shapes, and their good reproducibility in batch production open up wide possibilities in the application of such shells in intelligent micro- and nanosystems, and also in sensors and actuators. Other applications of 3D elastic nanostructures include sensors, actuators for MEMS/NEMS and smart systems based on such structures. The replacement of bulk sensor/actuator components with nanoshells drastically improves the sensitivity and response rate of the devices. Below, we give one example in which the replacement of a wire with an ultrathin-walled tube (1–100 nm) reduces the thermal inertia of a sensor or actuator by two orders of magnitude. This improves the response speed of sensors and actuators, allows the detection and suppression of rapidly developing turbulence, and assists the development of smart

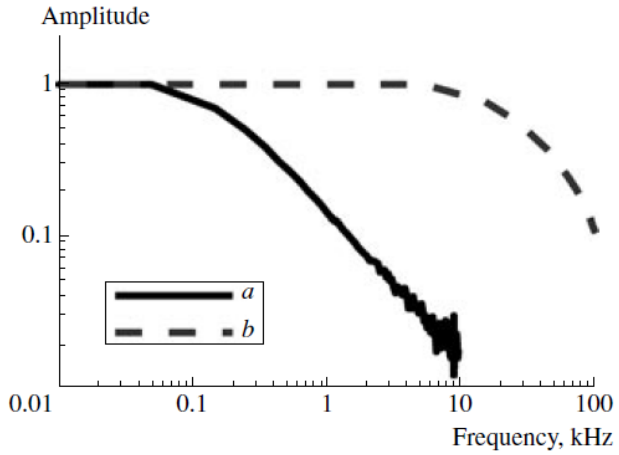

Figure 6. Amplitude–frequency characteristics of hot-wire (a) and hot-tube (b) sensitive elements. For the hot-tube probe, the time constant is 100 times smaller than that for the standard hot-wire probe, which enables us to considerably extend the frequency range of measurements and to study rapid processes that generate turbulence at high flow velocities [44, 45].

control systems providing a laminar flow regime around new aircraft.

The control of the laminar–turbulent transition in the boundary layer is a long-standing practical challenge in the field of gas dynamics and hydrodynamics. If solved, it will enable a significant reduction of drag for moving aircraft and the enhanced efficiency of air transport. The potential benefits of flow control include improved performance and maneuverability, affordability, increased range and payload, drag reduction, lift enhancement, mixing augmentation, heat-transfer enhancement and the suppression of flow-induced noise [39].

Recently, a prototype feedback control system for wall turbulence has been developed [40]. Arrays of micro hot-film sensors were employed to measure streamwise shear stress fluctuations, while arrays of magnetic actuators were used to introduce control input through wall deformation. A digital signal processor was employed to drive the actuators based on sensor signals. Feedback control experiments were performed in a turbulent air channel flow, and it was found that the wall shear stress (drag) could be decreased by up to 7%. A major deficiency of presently developed systems is a very long response time (∼ms), which restricts the application of such systems to low-velocity subsonic flow conditions [40, 41].

Heated wires, cooled by flowing gas, are widely used as flow sensors (hot-wire anemometry) [42]. In [43], it was shown that the replacement of hot wires with hot microtubes (see figure 6) improves the response time by a factor of 100. This property of tubular hot-wire sensors allows their use in supersonic flow systems operating at frequencies above 1 MHz.

In [44, 45], it was also shown that microtubes heated in a pulsed mode can be used as sensors and actuators; moreover, one and the same tube can be used as both a sensor and an actuator in smart turbulence control systems.

The tubular components are connected to control and readout devices using conductor lines located on the substrate (figure 7). The figure shows electron microscopy images of a chip with an array of hybrid microtubes rolled up from a $SiO_2/Si_3N_4/Au$ heterofilm. The total thickness of the walls in the $SiO_2/Si_3N_4/Au$ microtubes was 90 nm, and the tube diameter was about 10 μm.

The above example is suitable for gas-dynamics applications, with the tube wall thickness in the nanometer range and the tube diameter preset in the micrometer range. Because the shell technology can be scaled down to the nanometer region, the use of nanoscale hot-tube sensors and smart control systems based on such sensors is realistic in both hydrodynamic and nanofluidic applications.

5. Elements for micro- and nanofluidic MEMS/NEMS

Microfluidics and its applications to a lab-on-a-chip are described in [2]. The fundamentals of nanofluidics and the physics of liquid jets have been considered thoroughly in [46].

To deliver DNA and other biologically important molecules into a living cell, a micro-needle (or pipette) penetrating the membrane is used for microinjection [47]. However, the large pipette size and injection volume can damage cells. Smaller needle diameters (submicro- and nanometer) would enable new applications for these objects such as the handling and dissection of individual biological cells and chromosomes, and accurate microinjection into living cells.

The use of semiconductor technology in this field allows the mass production of such instruments. Many groups have conducted extensive research into the fabrication and application of micromachined microneedles [48–53]. Rolled-up tubes are also highly promising elements for the realization of nanofluidic MEMS/NEMS suitable for batch production. Indeed, rolled-up nanotubes with a broad range of lengths and diameters can be formed from semiconductors by a process perfectly compatible with planar and IC technologies.

Because of their very thin walls, rolled-up tubes offer much promise for use in microinjection systems. Rolled-up semiconductor microtubes were experimentally shown to possess a mechanical strength sufficient for the multiple piercing of plant cell walls [48, 49].

Below, an example is given in which structuring was achieved by the successive action of elastic forces. Figure 8 illustrates the formation of needles extending beyond the edge of a chip substrate. It can be clearly seen that the tubes are rolled at the first stage (a). At the second stage (b), the formed tubes become oriented upward under the action of internal elastic forces, thus forming a structure with a needle protruding over the substrate edge. Figure 8 shows examples of needles with atomically sharp edges, which were used for the development of micro- and nanosyringes and micro- and nanoneuroprobes [49].

An atomic-force microscope offers unrivaled running and positioning accuracy, which cannot be obtained using manual microactuators. The use of an atomic-force microscope for transfection was demonstrated for the first time in [54, 55]

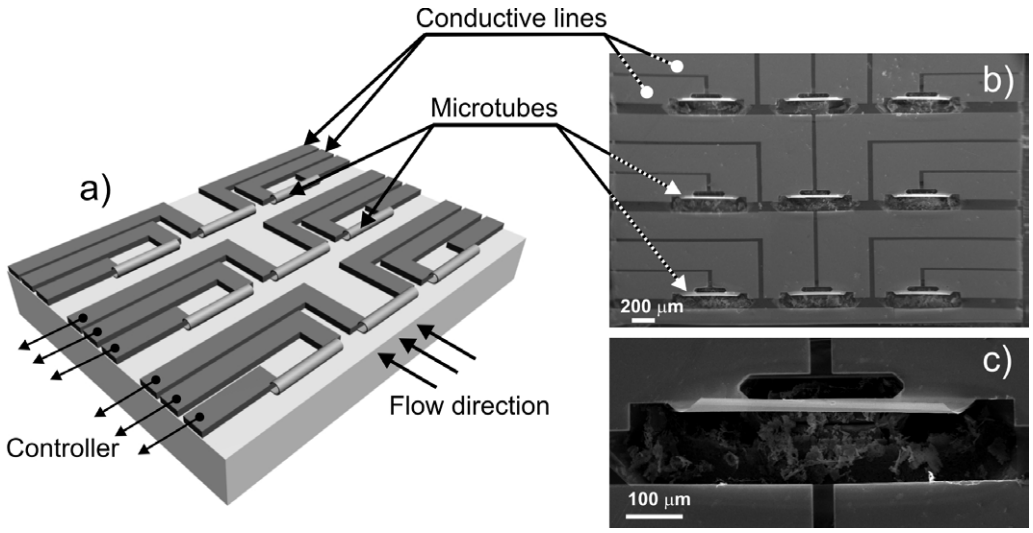

Figure 7. System of electrically conducting thin-walled microtubes with electrical contacts: (a) schematic of a chip with an array of microtubes; (b) SEM image of chip with microtubes fabricated from a $SiO_2/Si_3N_4/Au$ heterofilm (the tubes are suspended above the pits etched in the Si substrate); (c) enlarged image of one of the microtubes in (b) [44, 45].

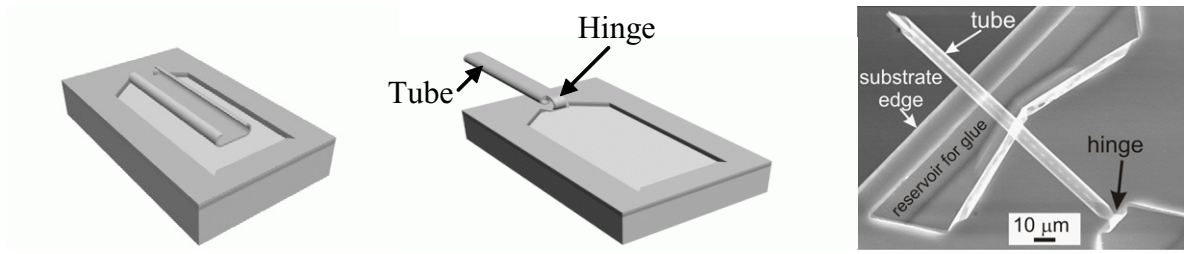

Figure 8. Formation of a tube protruding over the substrate edge. Scheme (a, b) and resultant Si/SiGe structure (c) [49].

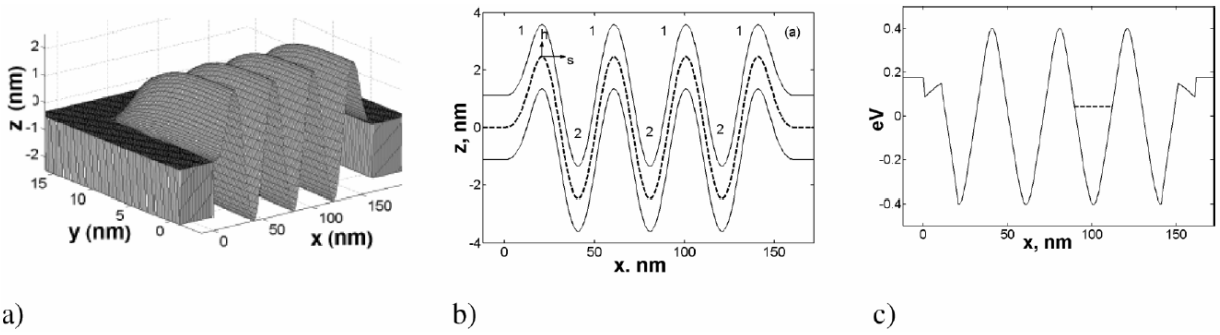

Figure 9. (a) Schematic view of a nanocorrugated structure. (b) Cross-section of the bilayer structure shown in (a): in the top layer, regions labeled 1 are under tensile stress, and regions labeled 2 are under compressive strain. (c) Confinement potential for electrons near the upper surface of the film (solid line) and the lower electron level (dashed line) [69].

using modified cantilevers with pointed tips. The microscope allows one to adjust the force applied to a cell and is therefore a very sensitive precision instrument. Several authors have used cantilevers modified with carbon nanotubes to puncture cell walls [57] and introduce molecules into living cells with the help of cantilever-mounted carbon nanotubes. The nanotubes were modified with a disulfide linker to fix a quantum dot covered with a protein [58]. It should be noted, however, that modified cantilevers and carbon nanotubes fixed at the needle point are rather costly to fabricate. In addition, such cantilevers cannot be used to dissect cells because they have no cutting edges.

Recently, we have fabricated cantilevers with tips, prepared as rolled-up tubes. Our initial experiments showed that rolled-up semiconductor nanotubes offer substantial advantages for cell puncture in comparison with carbon tubes.

Such tubes can be used for the development of nanojet printers [59]. In our experiment, a solution contained in

a microtube was locally heated by a resistive microheater prepared from Ni foil. Upon applying electric current pulses, the ink in the tube boiled locally, causing bubbles to form and liquid droplets to jet out of the tube. Minimum drop diameter of 100 nm was achieved using an inkjet prepared from a 200-nm diameter tube.

These examples demonstrate the potential capabilities of the technology in micro- and nanofluidic applications. These capabilities are based on the possibility of forming, using the new process, various nanoshells with perfectly controlled sizes that can be scaled down to nanometer region.

6. Building blocks for optical MEMS/NEMS

Extreme precision, a large variety of designs, wide-range scaling, the possibility of 3D arrangements and a parallel fabrication process make 3D shells ideal elements for various novel materials, particularly, for metamaterials, which present new opportunities for controlling electromagnetic radiation (for example, see reviews [60, 61]). 3D shells were used to create chiral structures and metamaterials in [62, 63]. Such shells can be used to create metamaterials with a negative index of refraction, and also magnetic and bianisotropic metamaterials that can control radiation over a wide spectral range, from microwaves to visible light. Arrays of precise hybrid metal-semiconductor helical microresonators were recently fabricated from strained bilayer films [63] (figures 1(d) and (e)). A maximum angle of polarization plane rotation in the microwave range (135–145 GHz) of 90° was achieved using an array of parallel helices oriented parallel to the wave direction, with a pitch close to the wavelength of microwave radiation. Giant rotation of the polarization plane of radiation by arrays of helices in the THz range was examined in [62, 63]. The elasticity and extreme shape stability of out-of-plane freely suspended shell resonators allow control of the shell shapes and the electromagnetic properties of shell-based metamaterials, respectively. The full compatibility of the method used with IC technology facilitates high-speed dynamic polarization control. The integration of shell helices with NEMS for the electromechanical control of helix geometry is very promising for the formation of solid-state metamaterials analogous to liquid crystals that can control radiation in different spectral ranges. Above, we considered 3D structures formed by thin films of nanometer thickness. Our recent experiments showed that the structuring method enabling the formation of 3D nanostructures can be successfully transferred to films of atomic thickness [64].

7. Prospects for NEMS with tunable quantum properties

Conducting nanoshells exhibit unusual quantum properties (see, for instance [65–69]), which can be further controlled by displacing parts of such elastic systems at the nanoscale.

There are a few strategies for providing mechanical systems with tunable quantum properties. The shuttle proposed in [65] is one of the most well-known mechanical systems employing quantum properties. Using such a shuttle, for instance, single-electron transfer can be achieved. We expect that shuttling devices for electrons can be fabricated using the above-discussed technology for 3D shells. Also, even simpler ways are presently available for the fabrication of NEMS with tunable quantum properties.

The conformal transformations of shells analogous to the conformal transformations of molecules that widely occur in nature are of much interest to us. Upon the modification of the molecular configurations, the molecular properties may also exhibit considerable changes [70].

Below, we describe the possibility of mechanically controlling shell shapes and, hence, the quantum properties of modified structures. In section 3 and in [12] we showed that under the action of electrostatic forces the corrugation configuration can undergo dramatic modifications, leading, for instance, to a sequential decrease in the corrugation period and film-bending radius.

When a film bends, its outer layers stretch and its inner layers compress, and the strain ε_s in the direction along the surface varies linearly across the film [71, 72]: $\varepsilon_s = h/R$, where h is the thickness of the film and R is its curvature radius calculated by differential geometry formulae. Calculations of a nanocorrugated structure [69] revealed that the film bends can produce deep quantum wells (up to 1 eV deep for thin InAs films). When an external action is exerted on such a corrugated film (see section 3), a system can be obtained with tunable quantum properties at room temperature.

The transformation of corrugated structures by applying an external force was demonstrated in [12, 36, 37]. Undoubtedly, complex shells that are reconfigurable by electrostatic forces will form a basis for novel NEMS.

8. Conclusion

We have described some novel applications of precise 3D shell structures (powerful electrostatic nanoactuators, ultrafast tubular anemometers for measuring gas flows, elements for micro- and nanofluidic MEMS/NEMS, optical MEMS/NEMS). We have presented examples of precisely fabricated MEMS/NEMS devices based on semiconductors, metals, and hybrid micro- and nanoshells. Novel sensors and actuators and smart materials are briefly described. Finally, we outlined prospects for achieving NEMS with tunable quantum properties.

Acknowledgments

This work was supported by the Russian Foundation for Basic Research and by the Russian Government (Federal Programs).

References

[1] Cleland A 2003 *Foundations of Nanomechanics* (Berlin: Springer)
[2] Bhushan B 2004 *Springer Handbook of Nanotechnology* (Berlin: Springer)

[3] Goddard W A III, Brenner D W, Lyshevski S E and Iafrate G J 2002 *Handbook of Nanoscience, Engineering, and Technology* (Boca Raton, FL: CRC Press)
[4] Li M, Tang H X and Roukes M L 2007 *Nat. Nanotechnol.* **2** 114
[5] Becker E W, Ehrfeld W, Hagmann P, Maner A and Munchmeuer B 1986 *Microelectron. Eng.* **4** 35
[6] Furuya K 2008 *Sci. Technol. Adv. Mater.* **9** 014110
[7] Prinz V Ya, Seleznev V A, Gutakovsky A K, Chehovskiy A V, Preobrazenskii V V, Putyato M A and Gavrilova T A 2000 *Physica* E **6** 828
[8] Prinz V Ya 2003 *Microelectron. Eng.* **69** 466
[9] Prinz V Ya 2006 *Phys. Status Solidi* b **243** 3333
[10] Wilson S *et al* 2007 *Mater. Sci. Eng.* R **56** 1
[11] Liu C 2007 *Adv. Mater.* **19** 3783
[12] Prinz A V and Prinz V Ya 2008 *Proc. 16th Int. Symp. on Nanostructures: Physics and Technology* pp 147–8
Prinz A V and Prinz V Ya 2006 *Russian Patent* No. 2278815
[13] Cho A 2006 *Science* **313** 164
[14] Scott S A and Lagally M G 2007 *J. Phys. D: Appl. Phys.* **40** R75
[15] Li X 2008 *J. Phys. D: Appl. Phys.* **41** 193001
[16] Prinz V Ya, Grutzmacher D, Beyer A, David C, Ketterer B and Deccard E 2001 *Nanotechnology* **12** 399
[17] Prinz A V and Vorob'ev A B 2002 *Semicond. Sci. Technol.* **17** 614
[18] Golod S V, Prinz V Ya and Mashanov V I 2005 *Thin Solid Films* **489** 169
[19] Prinz V Ya, Vorob'ev A B and Seleznev V A 2001 *Inst. Phys. Conf. Ser.* **170** 319
[20] Seleznev V A, Yamaguchi H, Hirayama Y and Prinz V Ya 2003 *Japan. J. Appl. Phys.* **42** L79
[21] Prinz V Ya, Chekhovskiy A V, Preobrazhenskii V V, Semyagin B R and Gutakovsky A K 2002 *Nanotechnology* **13** 231
[22] Zhang L, Abbott J J, Dong L, Kratochvil B E, Bell D and Nelson B J 2009 *Appl. Phys. Lett.* **94** 064107
[23] Grutzmacher D, Zhang L, Dong L, Bell D, Nelson B, Prinz A V and Ruhd E 2008 *Microelectron. J.* **39** 478
[24] Prinz V Ya and Golod S V 2006 *J. Appl. Mech. Tech. Phys.* **47** 867
[25] Nastaushev Yu V, Prinz V Ya and Svitasheva S N 2005 *Nanotechnology* **16** 908
[26] Luchnikov V, Sydorenko O and Stamm M 2005 *Adv. Mater.* **17** 1177
[27] Mei Y, Huang G, Solovev A, Bermudes E, Monch I, Ding A, Reindl T, Fu R, Chu P and Schmidt O G 2008 *Adv. Mater.* **20** 4085
[28] Bell D J, Dong L, Nelson B J, Golling M, Zhang L and Grützmacher D 2006 *Nano Lett.* **6** 725
[29] Nemirovsky Y and Degani O 2001 *J. Micromech. Syst.* **10** 601
[30] Degani O, Socher E, Lipson A, Leitner T, Setter D J, Kaldor S and Nemirovsky Y 1998 *J. Micromech. Syst.* **7** 373
[31] Bermejo S *et al* 2008 *J. Micromech. Microeng.* **18** 055004
[32] Seeger J I and Boser B E 2003 *J. Microelectromech. Syst.* **12** 656
[33] Li Y, Packirisamy M and Bhat R 2008 *Microsyst. Technol.* **14** 255–66
[34] Guo J G and Zhao Y P 2006 *Int. J. Solids Struct.* **43** 675
[35] Rollier A S *et al* 2006 *J. Micromech. Microeng.* **16** 794
[36] Prinz V Ya, Prinz A V and Kopylov A V 2008 *Patent Appl.* No. 208122800 favorable decision 14.04.2009
[37] Kopylov A V, Prinz A V and Prinz V Ya *to be published*
[38] Antonova I V, Soots R A, Guliaev M B, Prinz V Ya, Kagan M S and Kolodzey J 2007 *Appl. Phys. Lett.* **91** 102116
[39] Ikeda K 2007 *Sci. Technol. Trends—Q. Rev.* **22** 98
[40] Yoshino T, Suzuki Y and Kasagi N 2008 *J. Fluid Sci. Technol.* **3** 137
[41] Ho C-H and Tai Y-C 1998 *Annu. Rev. Fluid Mech.* **30** 579
[42] Hinze J O 1959 *Turbulence: An Introduction to its Mechanism and Theory* (New York: McGraw-Hill) p 680
[43] Fomin V M, Shiplyuk A N, Aniskin V M, Maslov A A, Pai V V, Prinz V Ya and Seleznev V A 2006 *Dokl. Phys.* **51** 132
[44] Seleznev V A, Prinz V Ya, Aniskin V M and Maslov A A 2009 *J. Appl. Mech. Tech. Phys.* **50** 291 (Engl. Transl.)
Seleznev V A, Prinz V Ya, Aniskin V M and Maslov A A 2009 *Prikl. Mekh. Tekh. Fiz.* **50** 145
[45] Shiplyuk A N, Aniskin M V, Seleznev A V, Prinz V Ya, Maslov A A and Matvienko A A 2009 *J. Appl. Mech. Tech. Phys.* **50** 454
[46] Eggers J and Villermaux E 2008 *Rep. Prog. Phys.* **71** 036601
[47] Anderson W F, Killos L, Sanders-Haigh L, Kretschmer P J and Diacumakos E G 1980 *Proc. Natl. Acad. Sci. USA.* **77** 5399
[48] Prinz A V and Prinz V Ya 2003 *Surf. Sci.* **532–535** 911
[49] Prinz V Ya, Golod S V and Prinz A V 2008 *Patent of Russia* No. 2341299
[50] Schrlau M *et al* 2008 *Nanotechnology* **19** 015101
[51] McAllister D V, Allen M G and Prausnitz M R 2000 *Annu. Rev. Biomed. Eng.* **2** 289
[52] Reed M L and Lye W K 2004 *Proc. IEEE* **92** 56
[53] Lin L W and Pisano A P 1999 *J. Microelectromech. Syst.* **8** 78
[54] Han S W *et al* 2005 *Biosens. Bioelectron.* **20** 2120
[55] Han S W *et al* 2008 *Nanomed.: Nanotechnol. Biol. Med.* **4** 215
[56] Obataya I *et al* 2005 *Nano Biotechnol.* **1** 347
[57] Vakarelski I U, Brown S C, Higashitani K and Moudgil B M 2007 *Langmuir* **23** 10893
[58] Chen X, Kis A, Zettl A and Bertozzi C R 2007 *Proc. Natl. Acad. Sci. USA* **104** 8218
[59] Prinz A V, Prinz V Ya and Seleznev V A 2003 *Microelectron. Eng.* **67–68** 782
[60] Lapine M and Tretyakov S A 2007 *IET Microw. Antennas Propag.* **1** 3
[61] Pendry J B and Smith D R 2006 *Sci. Am.* **295** 60
[62] Naumova E V *et al* 2009 *J. Opt. A: Pure Appl. Opt.* to be published in a special issue
[63] Naumova E V and Prinz V Ya 2008 *Russian Patent* No. 2317942
[64] Prinz V Ya and Seleznev V A 2007 *Phys. Status Solidi* b **244** 4193
[65] Shekhter R I, Galperin Yu, Gorelik Y L, Isacsson A and Jonson M 2003 *J. Phys.: Condens. Matter* **15** R441
[66] Vorob'ev B, Friedland K-J, Kostial H, Hey R, Jahn U, Wiebicke E, Yukecheva Ju S and Prinz V Ya 2007 *Phys. Rev.* B **75** 205309
[67] Kibis O V and Portnoi M E 2007 *Tech. Phys. Lett.* **33** 878
[68] Magarill L I and Éntin M V 2003 *JETP Lett.* **78** 213
[69] Prinz A V and Prinz V Ya 2006 *Russian Patent* No. 2278815
[70] Osadchii V M and Prinz V Ya 2005 *Phys. Rev.* B **72** 033313
[71] Tsui Y C and Clyne T W 1997 *Thin Solid Films* **306** 23
[72] Timoshenko S and Woinowsky-Krieger S 1959 *Theory of Plates and Shells* (New York: McGraw-Hill)